

Supplementary material

Supplementary material

High-performance energy-storage ferroelectric multilayer ceramic capacitor via nano-micro engineering

Ziyue Ma¹, Yong Li^{1,*}, Ye Zhao¹, Ningning Sun¹, Chunxiao Lu¹, Pei Han¹, Dawei Wang^{2,3,*}, Yanhua Hu⁴, XiaoJie Lou⁵, Xihong Hao^{1,*}

¹Inner Mongolia Key Laboratory of Ferroelectric-Related New Energy Materials and Devices, School of Materials and Metallurgy, Inner Mongolia University of Science and Technology, Baotou 014010, China

²Shenzhen Institute of Advanced Electronic Materials, Shenzhen Institute of Advanced Technology, Chinese Academy of Sciences, Shenzhen 518055, China

³Functional Materials and Acousto-Optic Instruments Institute, School of Instrumentation Science and Engineering, Harbin Institute of Technology, Harbin 150080, China

⁴Department of Chemical Engineering, Ordos institute of technology, Erdos 017000, China

⁵Frontier Institute of Science and Technology, and State Key Laboratory for Mechanical Behavior of Materials, Xi'an Jiaotong University, Xi'an 710049, China

*Corresponding author. E-mail: liyong3062545@126.com; wangdawei102@gmail.com; xihonghao2022@163.com.

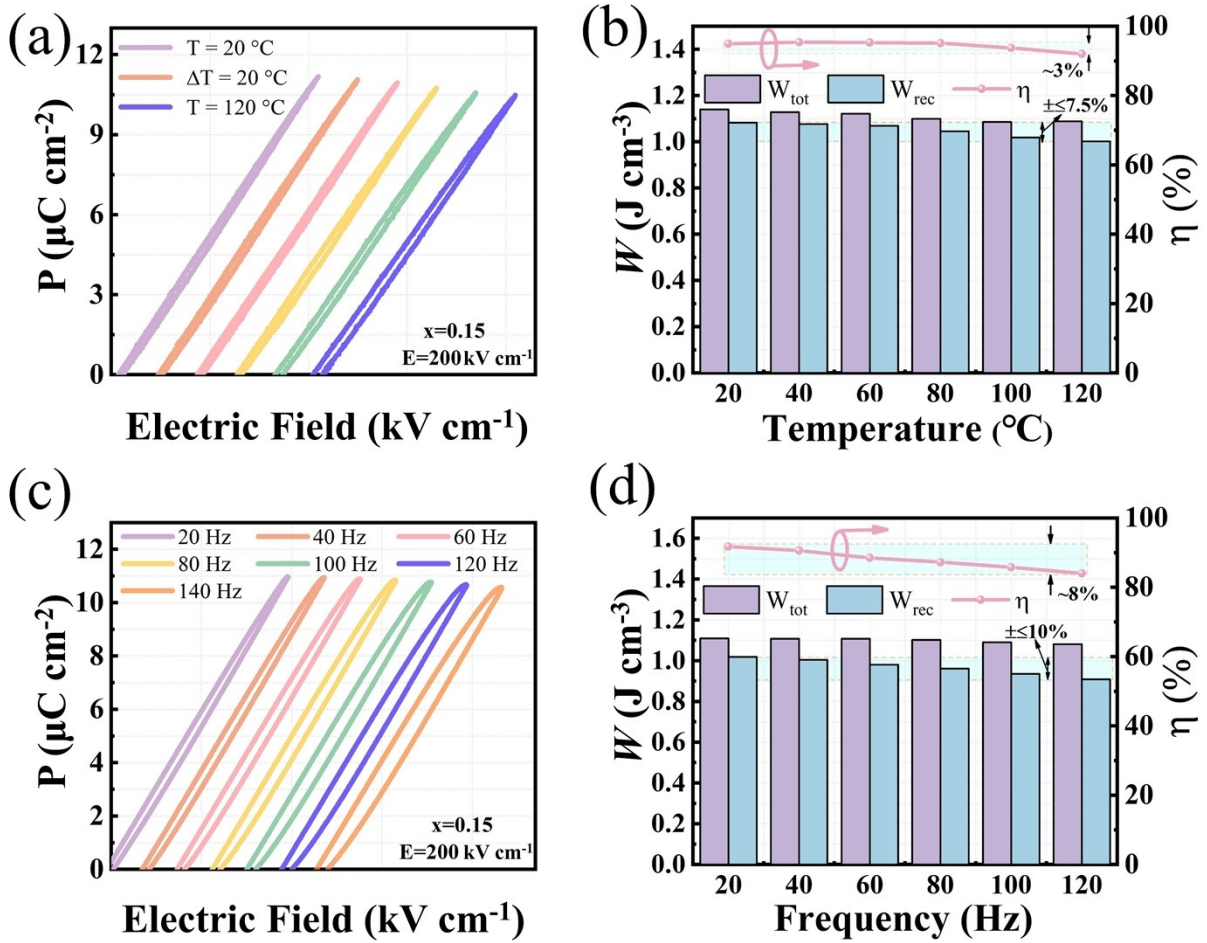


Fig. S1. P - E loop of $x=0.15$ ceramic as a function of (a) temperature, (c) frequency. (b) The temperature dependent, (d) the frequency dependent W_{tot} , W_{rec} and η of $x=0.15$.

Supplementary material

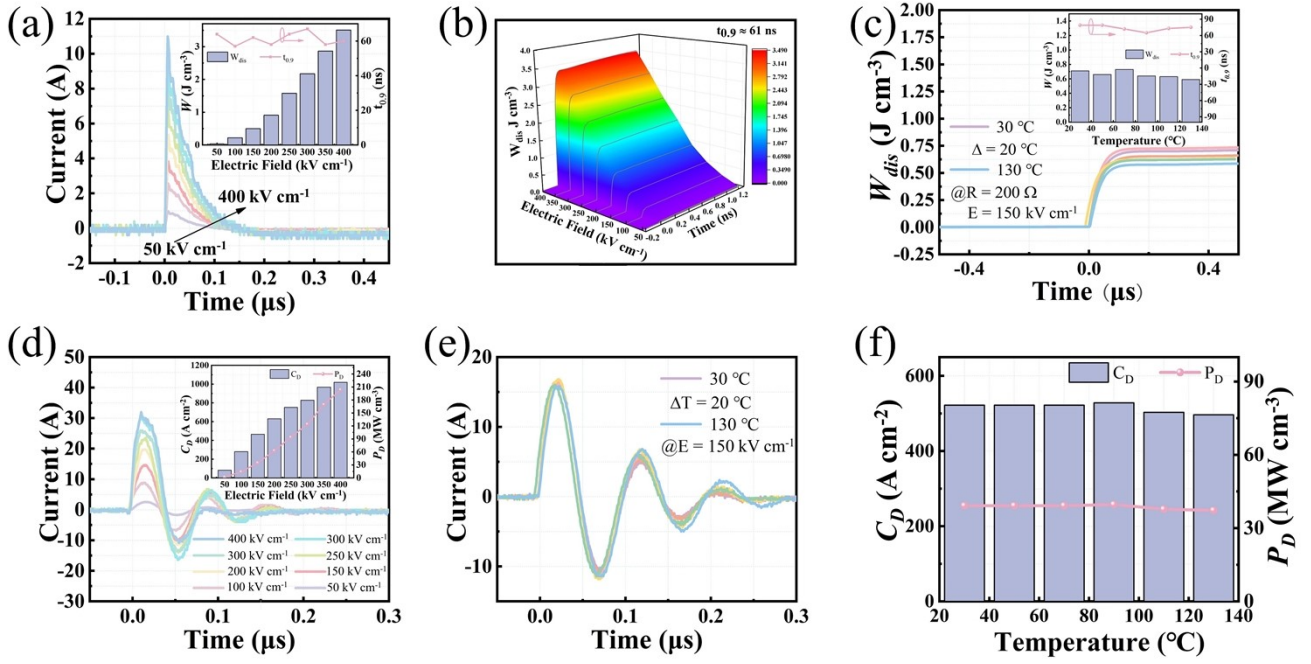


Fig. S2. (a-b) The discharge current waveform, W_{dis} and $t_{0.9}$ of x=0.15 ceramic in the overdamped state at different electric fields and the inset shows the corresponding W_{dis} and $t_{0.9}$. (c) The W_{dis} of x=0.15 ceramic in the overdamped state at different temperatures and the inset shows the corresponding W_{dis} and $t_{0.9}$. (d) The discharge current waveform of x=0.15 ceramic in the underdamped state at different electric fields and the inset shows the corresponding C_D and P_D . (e-f) The discharge current waveform, C_D and P_D of x=0.15 ceramic in the underdamped state at different temperatures.

Supplementary material

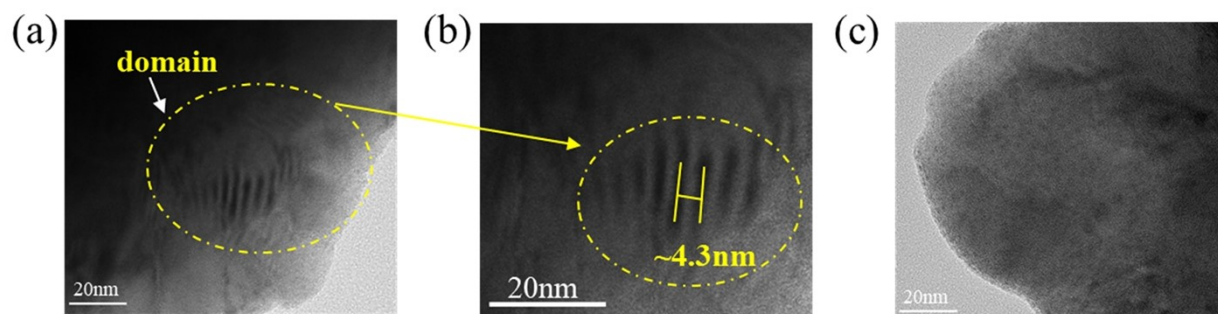


Fig. S3. TEM images of (a-b) $x=0.05$ and (c) $x=0.2$.

Supplementary material

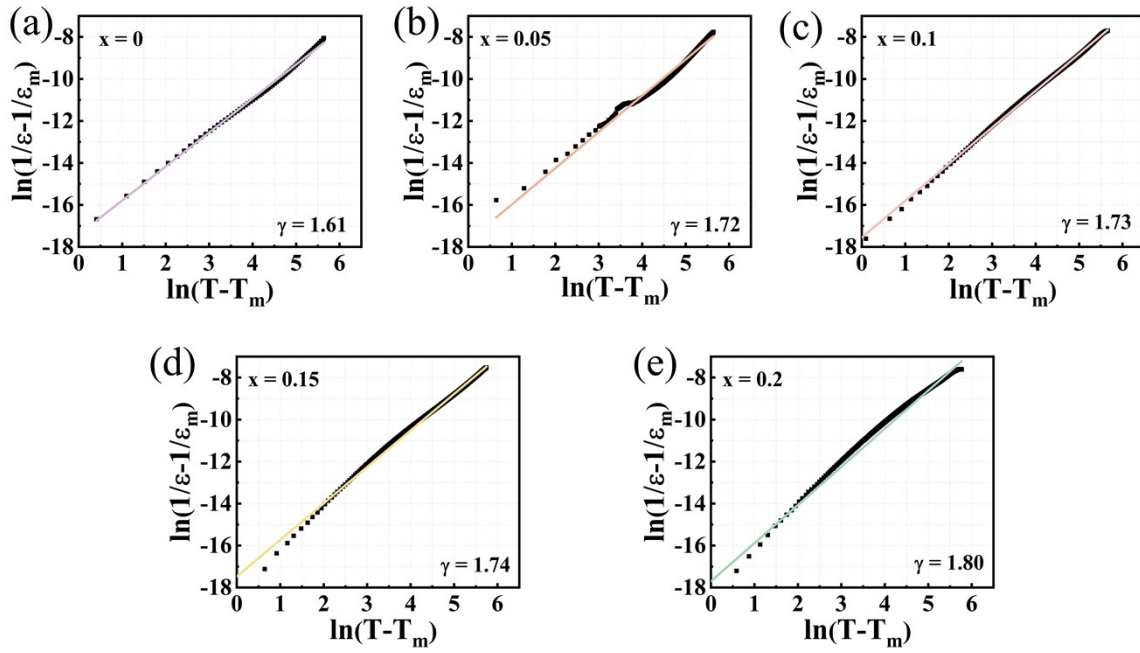


Fig. S4. The $\ln(1/\epsilon_r - 1/\epsilon_m)$ varies with $\ln(T - T_m)$ of $(1-x)(0.65\text{NBT}-0.35\text{ST})-x\text{LMZ}$ ceramics (a) $x=0$, (b) $x=0.05$, (c) $x=0.1$, (d) $x=0.15$, (e) $x=0.2$.

Supplementary material

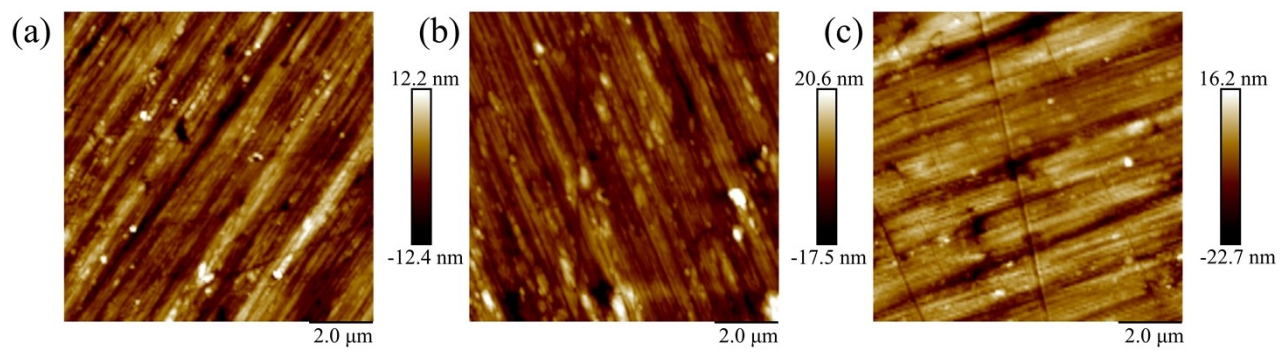


Fig. S5. The topography pictures of: (a) $x=0$, (b) $x=0.10$ and (c) $x=0.15$ ceramics.

Supplementary material

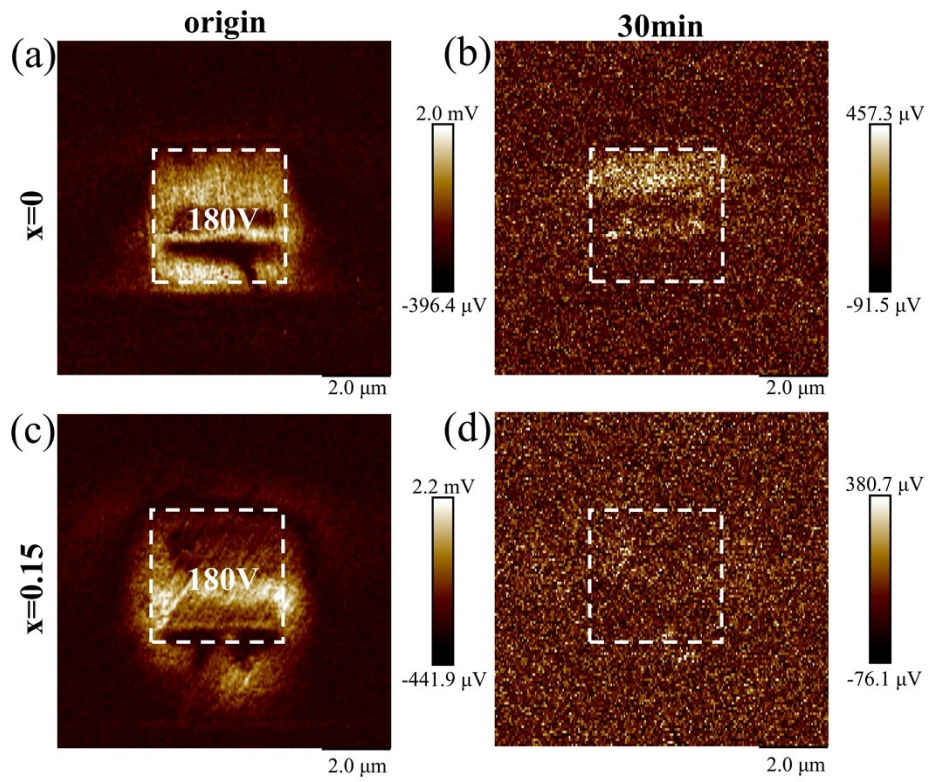


Fig. S6. Out-of-plane PFM amplitude pictures and domains evolution under different times for (a-b) $x=0$ and (c-d) $x=0.15$ ceramics.

Supplementary material

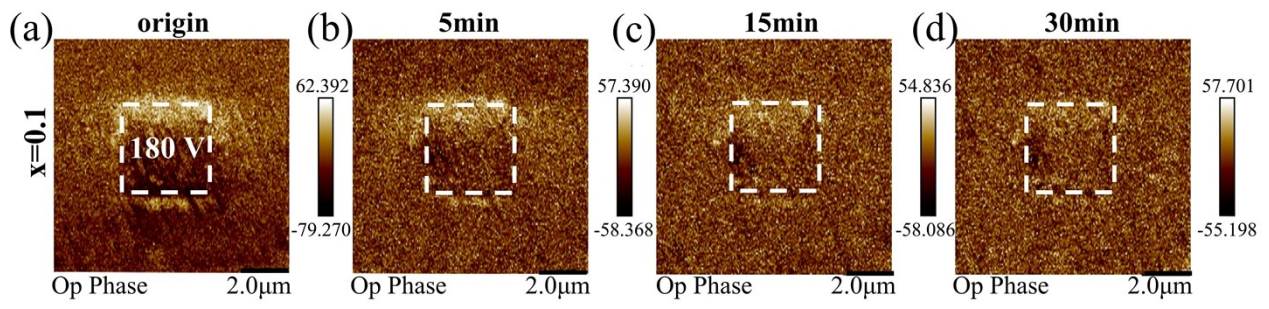


Fig. S7. Out-of-plane PFM phase pictures and domains evolution under different times for $x=0.1$ ceramics.

Supplementary material

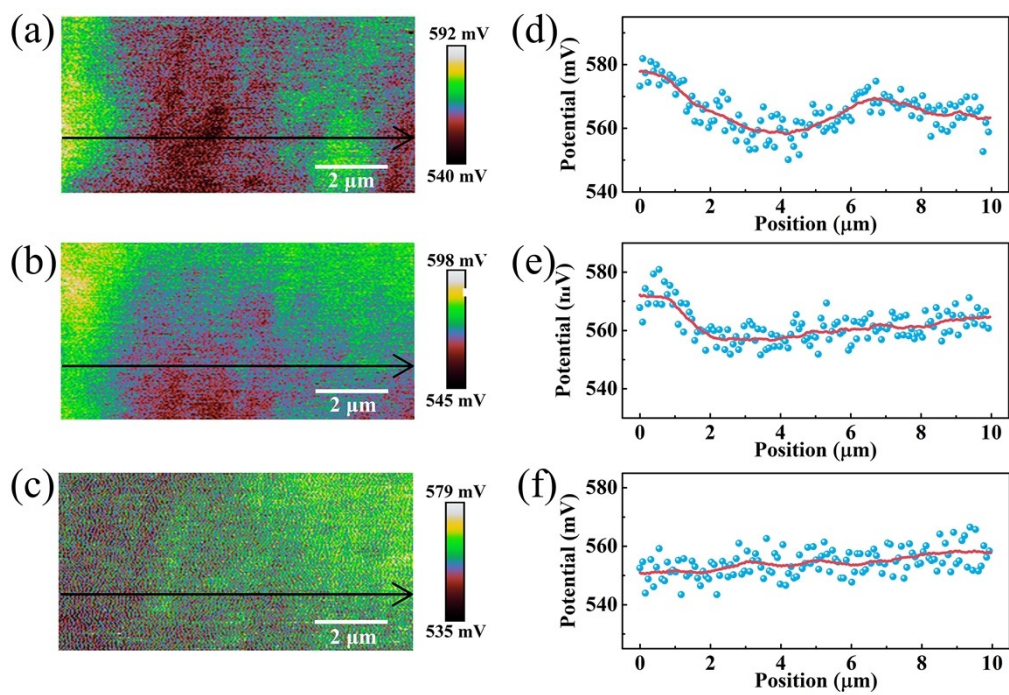


Fig. S8. Potential maps, and potential profile of (a,d) $x=0.05$, (b,e) $x=0.10$ and (c,f) $x=0.2$.